

Domain Shape Transitions in Emulsified Polyolefin Blends

H. S. Jeon, J. H. Lee, and N. P. Balsara*

Department of Chemical Engineering, Polytechnic University, Six Metrotech Center, Brooklyn, New York 11201

B. Majumdar

Corporate Research Process Technologies Laboratory, 3M Company, Building 208-1-01, St. Paul, Minnesota 55144

L. J. Fetters

Corporate Research Laboratories, Exxon Research and Engineering Company, P.O. Box 998, Clinton Township, Annandale, New Jersey 08801-0998

A. Faldi

*Polymer Science Division, Exxon Chemical Company, 5200 Bayway Drive, Texas 77522**Received August 14, 1996; Revised Manuscript Received December 19, 1996*

ABSTRACT: The shape of dispersed domains in emulsified polyolefin blends was studied by transmission electron microscopy. Model polyolefins—polyethylene (PE), head-to-head polypropylene (PP), and PE–PP diblock copolymers—were synthesized via anionic polymerization. Ternary blends with PE as the minor component were studied at 200 °C. All components are amorphous at this temperature. We find that increasing $\phi_{\text{PE-PP}}/\phi_{\text{PE}}$ at constant $\phi_{\text{PE-PP}} + \phi_{\text{PE}}$ leads to an abrupt transition from spherical domains to cell-like domains with faceted walls (where ϕ_i is the volume fraction of component i). However, the cell-like domains were aggregated and formed large macrophases. The characteristic size of the domain-rich phase was considerably larger than the size of the PE droplets formed in the absence of the block copolymer. This indicates strong adhesive interactions between the cell-like domains. Current theories on emulsified polymer blends ignore interdomain interactions.

Introduction

Amphiphiles such as surfactants and block copolymers are often used to create stable dispersions of immiscible liquids. These mixtures are called microemulsions. Surfactants are used to create oil domains in water,¹ while block copolymers are used to create domains of one polymer in another.² We use the term “domains” instead of droplets or globules because the dispersed phase can assume nonspherical as well as spherical shapes.¹ The amphiphiles are preferentially located at the domain–matrix interface, and this stabilizes the dispersion. It is believed that the underlying forces that determine the size and shape of the domains in small molecule systems and polymeric systems are similar.^{1,3,4} However, predicting the state of these multicomponent mixtures is challenging due to the fact that these systems possess many degrees of freedom. A variety of domain shapes such as spheres, cylinders, and lamellae have been identified.^{1–4} The interface between the domain and the matrix is flexible to varying degrees, and this leads to configurational freedom. Sometimes domains with different shapes can coexist with each other. Further, attractive interdomain interactions may cause macrophase separation, leading to coexisting domain-rich and domain-poor phases.⁵

For a given mixture, the structure and organization of the domains is determined by a variety of intermolecular and intramolecular factors. Intermolecular interactions can be gauged by studying the (three) binary phase diagrams of the constituents.⁶ Intramolecular factors, particularly the architecture of the amphiphile, dictate the properties of the domain–

matrix interface, such as spontaneous curvature and bending moduli.^{1–6} In the case of polymeric amphiphiles, these properties can be predicted on the basis of chain statistics.⁷ Such predictions are not possible for small molecule amphiphiles where these parameters depend on molecular details.^{1,4}

In this paper we study the structure of microemulsions formed in ternary mixtures of two homopolymers and a diblock copolymer by transmission electron microscopy. Model polyolefins—polyethylene (PE), head-to-head polypropylene (PP), and PE–PP diblock copolymers—were synthesized via anionic polymerization. All three components used in this study are aliphatic hydrocarbons with empirical formula CH_2 . We thus expect intermonomer interactions to be purely dispersive in origin, and the thermodynamics of mixing are expected to be consistent with the Flory–Huggins theory.^{8,9} In this theory, intermolecular interactions are determined by a single parameter, χ . This theory is adequate for a variety of binary polyolefin blends.¹⁰ A recent study has shown that thermodynamic data from multicomponent polyolefin blends are also consistent with the Flory–Huggins theory.¹¹

Wang and Safran have proposed a thermodynamic model for predicting the structure of polymer microemulsions where intermolecular interactions are described by the Flory–Huggins theory.⁴ The approach used by these authors was pioneered by Leibler.³ The shape of the domains is predicted to change from spheres to cylinders and from cylinders to lamellae as the block copolymer concentration is increased. This is shown schematically in Figure 1. The theory provides explicit predictions for the transition points in terms of variables that can be measured independently.

Our objective is to examine the possibility of domain shape transitions in PE/PP/PE–PP blends. The molec-

* Abstract published in *Advance ACS Abstracts*, February 1, 1997.

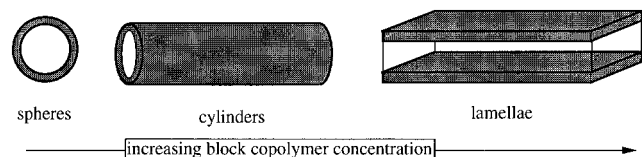


Figure 1. Schematic representation of domain shapes predicted by Wang and Safran.⁴ The shaded region represents the block copolymer layer that is assumed to coat the minor phase. The unshaded regions in the interior of the coat represent the minor phase. The topology of the block copolymer "caps" at the edges of the cylindrical and lamellar domains is not specified in the theory and is not shown in the drawing.

ular weights of the components were chosen so that the blends were strongly phase separated. This paper is part of a series on thermodynamics and phase transitions in multicomponent polymer blends.^{11–14} Our previous studies were restricted to single-phase blends^{11,12} and weakly phase-separated blends in the vicinity of phase transition temperatures.^{13,14}

The morphology of mixtures of two homopolymers and a block copolymer have been studied extensively (for example, see refs 2 and 15–19). These studies are largely motivated by the commercial success of materials such as high-impact polystyrene in which a dispersed polybutadiene phase is stabilized by polystyrene-polybutadiene graft copolymers. The complexity of the phase diagrams in these systems was demonstrated by early experiments of Ramos and Cohen.¹⁵ While the interfacial activity of the graft copolymers has been established in several systems,² many fundamental questions about the physical origin of their properties are still being debated.^{16–19} To our knowledge, a quantitative understanding of the factors that govern the shape and size of the dispersed phase domains does not exist.

Experimental Methods and Material Characterization

Nearly monodisperse, model polyolefins were synthesized in two steps.²⁰ First, diene monomers were polymerized anionically under high vacuum in hydrocarbon solvents at 25 °C with *sec*-butyllithium as the initiator and 2-propanol as the terminator. Standard high-vacuum procedures were used to purify the reagents.²¹ Under these conditions dienes are expected to polymerize primarily by 1,4-addition. Second, separate portions of the polydiene were saturated with H₂ in cyclohexane under pressure (500 psi), at 100 °C, in the presence of a palladium catalyst. Butadiene and 2,3-dimethylbutadiene were used as monomers to yield polyethylene (PE) and head-to-head polypropylene (PP).



head-to-head polypropylene (PP)

polyethylene (PE)

Two PE-PP diblock copolymers were synthesized under identical conditions, by sequential addition of the butadiene followed by 2,3-dimethylbutadiene. An aliquot of the polybutadiene precursor was isolated and terminated for characterization purposes, prior to the addition of the 2,3-dimethylbutadiene. The molecular weights of the polymers were determined by low-angle light scattering at 135 °C using 1,2,4-trichlorobenzene as the solvent. The refractive index increment (dn/dc) was assumed to be $-0.104 \text{ cm}^3/\text{g}$, which applies to both polyethylene and polypropylene.²² The molecular weights of the homopolymers were confirmed by conducting light scattering measurements on cyclohexane solutions of the diene precursors. The polydispersity index of the polymers was estimated from GPC measurements on THF solutions of

Table 1. Characterization of Polymers

sample	molecular weight (g/mol) ^a	mol % 1,4-addition ^b	vol fr of PE in block copolymers ^b (<i>f</i>)
PE	5.9×10^4	92	
PP	1.0×10^5	>96 ^c	
PE-PP[45–90]	1.35×10^5	PE, 89; PP, 76	0.34
PE-PP[115–65]	1.80×10^5	PE, 89; PP, 74	0.62

^a Light scattering. ^b Based on ¹H NMR on polydienes. ^c Beyond detection limit.

the polydienes and was less than 1.20 in all cases. The percentage of 1,4-addition and the composition of the copolymers were determined from ¹H NMR measurements on solutions of the polydiene block copolymers. High-temperature ¹³C NMR on the polyolefins (120 °C in tetrachloroethane-*d*₂) was used to confirm the block copolymer compositions. The spectroscopic measurements confirmed complete (>97%) saturation of the double bonds.

The characteristics of the polymers used in this study are listed in Table 1.²³ The block copolymers are labeled according to the molecular weights of the PE and PP blocks in kg/mol. PE is the minor component in one of the copolymers, while PP is the minor component in the other copolymer. The percentage of 1,4-addition in the PE blocks in the copolymers as well as that in the PP and PE homopolymers is in the vicinity of 90% or greater. This is typical of polydienes synthesized by anionic polymerization in hydrocarbon solvents. In contrast, the percentage of 1,4-addition in PP blocks of both the copolymers is in the vicinity of 75 mol %. We do not know what caused this relatively high incorporation of 1,2-units in the PP blocks. On the basis of current knowledge of polymer-polymer interactions, we do not expect the mismatch in the 1,4-content to have a significant effect on the thermodynamics of PE/PP/PE-PP blends.²⁴

Multicomponent mixtures were prepared by solution blending. We started with a dilute solution (1 wt % total polymer) containing the appropriate amounts of PE, PP, and PE-PP in toluene. The mixture was stirred and heated from room temperature to 108 °C in 90 min, at which point the toluene began to boil. All the polymers were soluble in boiling toluene. The mixture was kept at 108 °C for 15 min and then poured quickly into a 50/50 methanol/acetone mixture at room temperature. This resulted in the formation of a white precipitate, which was transferred into glass cuvettes. The blends were dried in a vacuum oven by slowly increasing the oven temperature from room temperature to 200 °C in about 2 h. This resulted in a dry melt which was further annealed at 200 °C for 14 h. Increasing the annealing time to 20 h and removing the samples from the oven at intermediate times and reheating them had no effect on the blend morphology. After annealing, the samples were rapidly quenched using liquid N₂ and kept there for 30 min. Our objective was to "freeze" the structure at 200 °C. The cuvettes were then brought to room temperature and heat sealed. The samples were stored at room temperature.

The blends were removed from the cuvettes (typically 1 week after the annealing step), and thin (30 nm in thickness) sections were obtained using a Reichert Ultramicrotome at -120 °C. Most of the samples were stained with RuO₄ and examined on a Jeol 1210 transmission electron microscope. The staining is not entirely necessary, due to the natural electron contrast between PE and PP at room temperature. Consequently, some samples were studied without staining.

The compositions of the blends examined in this work are listed in Table 2. All the blends were phase separated, and PE was always the minor homopolymer component. The compositions of the blends are specified by two variables: $w = \phi_{\text{PE-PP}}/\phi_{\text{PE}}$ and $\phi = \phi_{\text{PE-PP}} + \phi_{\text{PE}}$ (ϕ_i is the volume fraction of component *i*). The volume fractions were calculated using the measured weight fractions, using the amorphous densities²⁵ of the components at room temperature, and assuming no volume change on mixing. In the case of PE and PE-PP copolymers, the amorphous density was estimated using the data in ref 26.

The theories that we wish to address^{3,4} are based on equilibrium thermodynamics. We designed the blend prepara-

Table 2. Composition of Blends Discussed in This Paper

blends shown in	ϕ	w
Figure 2 (binary)	0.10	0
Figures 4 and 5 (ternary with PE-PP[45-90])	0.05	0.53
	0.05	1.39
	0.05	2.35
	0.05	3.06
	0.05	3.23
	0.05	3.69
	0.10	2.34
	0.10	3.23
	0.10	3.24
	0.16	2.35
	0.22	2.35
	0.22	1.41
	0.27	3.28
	0.28	2.18
Figure 7 (ternary with PE-PP[115-65])	0.05	1.40
	0.05	1.96
	0.05	3.24
	0.33	3.24

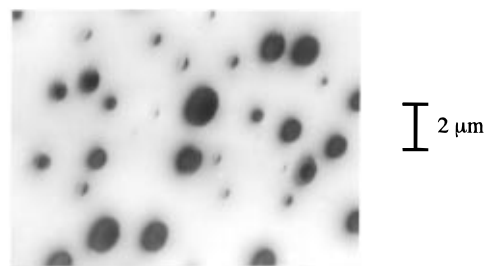
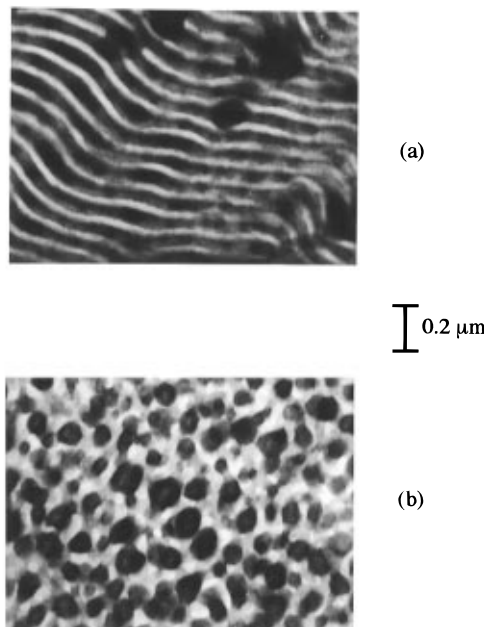
tion method to try and ensure that the observed domains were at equilibrium. Presumably, the solution blending and precipitation procedure led to an intimate mixture of PE, PP, and PE-PP. The rate of formation of the PE-rich domains thus depends on diffusion, i.e., the longest relaxation time of the individual chains, τ . The annealing times used in this study were much larger than τ . We estimate τ at the annealing temperature of 200 °C from the viscoelastic data of Graessley and co-workers.^{27,28} At 200 °C the zero shear viscosities of the homopolymers PE and PP (η_0) are 6.4×10^3 and 1.9×10^4 P, respectively. For entangled polymers, the longest relaxation time is given by $\tau = 12\eta_0/\pi^2 G_n^0$, where G_n^0 , the plateau modulus of PE and PP melts, is 2.6 and 0.52 MPa, respectively.²⁹ Using this relationship, we estimate that τ is 3.0×10^{-4} s for PE and 4.4×10^{-3} s for PP. It is more difficult to estimate τ for the block copolymers, but we expect it to be within 2 orders of magnitude of the homopolymer values. The annealing time used in this study is at least 7 orders of magnitude larger than the longest relaxation time of the molecules. During this time, the molecules are expected to diffuse across distances much larger than their radii of gyration, R_g . Fetters et al. have measured the molecular weight dependence of the radii of gyration (R_g) for PE and PP chains.²⁹ Using the scaling laws reported in ref 29, we estimate that $R_g = 11.1$ nm for PE and $R_g = 10.7$ nm for PP. There thus appears to be adequate time for the molecules to organize into equilibrium structures with characteristic sizes of a few microns. We also made modest changes in the sample preparation method (see above) and found no effect on the final morphology. This is a necessary, but not sufficient, condition for equilibrium.

Coarsening by domain coalescence during storage at room temperature can occur because the matrix phase (PP) is in the rubbery state. However, we estimate this to be negligible. The zero shear viscosity of the PP at room temperature is 8×10^8 P.²⁸ The size of the dispersed phase was found to vary between 0.1 and 10 μm . Using the Stokes-Einstein law, we estimate that the diffusion distance for the smallest domains is about 10^{-2} μm in 1 month.

From the considerations given above, we believe that the TEM micrographs represent the morphology of the blends at 200 °C after extensive annealing. All the components are amorphous and in the rubbery state at this temperature.

We conclude this section by reporting the characteristics of a binary PE/PP blend and the pure block copolymers, as revealed by electron microscopy. The thermal history of these samples was identical with that of the ternary blends discussed above. These experiments provide the necessary background for studying the emulsification of multicomponent blends.

The micrograph obtained from a PE/PP blend with $\phi_{\text{PE}} = 0.1$ ($\phi = 0.1$, $w = 0$) is shown in Figure 2. This sample was not stained. It is evident that the two polymers are immiscible at the measuring temperature of 200 °C. PE has a higher electron density, and hence the PE-rich regions appear dark in the figure. Staining this blend with RuO₄ results in an

**Figure 2.** Transmission electron micrograph of a binary PE/PP blend with $\phi_{\text{PE}} = 0.10$. The sample was examined without staining, and the dark regions represent the PE domains.**Figure 3.** Transmission electron micrographs of (a) PE-PP-[45-90], which shows a cylindrical morphology, and (b) PE-PP-[115-65], which shows a bicontinuous morphology. These samples were stained with RuO₄ which renders the PP mesophase dark.

increase in the electron density of the PP-rich matrix, thereby reducing the contrast between the coexisting phases. We find that the dispersed phase is spherical and the apparent diameter of the spheres ranges from 0.2 to 2 μm . The wide distribution of particle sizes that is observed is partly due to stereology and partly due to phase separation and coarsening processes. Coarsening can occur by either Ostwald ripening or coalescence. However, all the particles appear spherical, indicating that the return to sphericity after coalescence occurs relatively rapidly.

The micrographs obtained from the block copolymers are shown in Figure 3. These samples were stained with RuO₄ which preferentially attacks the amorphous, PP mesophase. A typical micrograph from PE-PP[45-90] is shown in Figure 3a. The microstructure is consistent with a cylindrical morphology. A typical micrograph obtained from PE-PP[115-65] is shown in Figure 3b. The sample appears to have a bicontinuous morphology. Recent experiments have shown that establishing the correct symmetry of bicontinuous block copolymer mesophases is not straight forward and requires a combination of scattering and TEM.³⁰ Also, the morphology of ordered, semicrystalline block copolymers can be distorted by crystallization, and the kinetics of these processes are not understood.³¹⁻³⁴

Establishing the TEM signatures of the pure block copolymers is useful because it allows us to identify pure block copolymer phases in the ternary mixtures, if they exist. These experiments also give a direct measure of the block copolymer chain dimensions. It is well known that block copolymer chains adopt stretched configurations when the junctions between the blocks are confined to interfaces.³⁸⁻⁴⁰ In pure,

Table 3. Domain Shape Transition Points Predicted by Wang and Safran⁴

domain shapes	w range	
	PE-PP[45-90] ($f = 0.34$)	PE-PP[115-65] ($f = 0.62$)
spheres	< 1.86	
coexisting spheres and cylinders	$1.86 < w < 2.16$	no predictions
cylinders	$2.16 < w < 2.77$	
coexisting cylinders and lamellae	> 2.77	

ordered block copolymers, the junctions are confined to the interface between the mesophases, while in emulsified blends they are confined to the domain-matrix interface. We therefore expect chain stretching in both cases. The average d -spacing in PE-PP[45-90] is $0.085 \mu\text{m}$, while that in PE-PP[115-65] is $0.100 \mu\text{m}$. Assuming that the radius of gyration (R_g) of the copolymers is given by $(R_{g,\text{PE}}^2 + R_{g,\text{PP}}^2)^{1/2}$, the (unperturbed) R_g of PE-PP[45-90] chains is estimated to be $0.014 \mu\text{m}$ while that of PE-PP[115-65] is estimated to be $0.018 \mu\text{m}$.²⁷ The extent of chain stretching in the ordered structures relative to the unperturbed state, given by $d/2R_g$, is 3.0 for PE-PP[45-90] and 2.8 for PE-PP[115-65].

Theoretical Background

We begin this section by summarizing the pertinent results of the Wang-Safran theory.⁴ Although the theory is quite general and can be applied to a variety of systems, the results simplify considerably in the limit of highly incompatible systems where $\chi \gg 1/N$. The quantity χ is the Flory-Huggins interaction parameter between PE and PP monomers, N is the number of repeat units per polymer chain for the smallest of the three molecules, and both χ and N are based on the same reference volume. In this limit, the domain shape is predicted to depend on two parameters: w , the relative concentration amphiphile to minor component, and f , the volume fraction of the minor homopolymer component in the block copolymer (PE in our case). The domain shape is independent of all other parameters such as total molecular weight of the components and χ . The equilibrium domain shapes under a given condition represent a compromise between curvature constraints due to homopolymer ratio ($\phi_{\text{PE}}/\phi_{\text{PP}}$) and the spontaneous curvature of the PE-PP block copolymers.

Most of our experiments were conducted on blends with PE-PP[45-90] as the surfactant. In this copolymer, $f = 0.34$. The values of w at which the spheres-to-cylinders (w_{sc}) and cylinders-to-lamellae (w_{cl}) transitions are predicted to occur are given in Table 3. The spontaneous curvature of the block copolymer decreases as f varies from 0.25 to 0.5, and this in turn favors the formation of cylindrical and lamellar domains. Thus, w_{sc} and w_{cl} decrease with increasing f , and they approach 0 as f approaches 0.5. Domain shapes in blends containing block copolymers with f greater than 0.5 are interesting because in order to coat the minor component, the block copolymer must adopt a conformation that is opposite to its spontaneous curvature. To study this regime we made some blends with PE-PP[115-65] which has $f = 0.62$. We are not aware of any predictions of domain shapes in systems with $f > 0.5$.

We note in passing that theories on microemulsion formation^{3,4} are qualitatively different from those based on the random phase approximation (RPA),³⁵⁻³⁷ which are now used routinely to study the thermodynamics of disordered block copolymers and homopolymer/block copolymer mixtures. The analysis of our previous experiments on multicomponent polymer blends¹¹⁻¹⁴ was based on the RPA.

The neglect of interdomain interactions is a key simplifying assumption in the Wang-Safran model. In polymeric systems, there is reason to question the validity of this assumption. The outer block of the copolymer coat on the domains (the PP block in our case) is similar to an end-adsorbed polymer brush. Interactions between polymer brushes have been studied extensively (e.g., refs 38-41). Self-consistent field calculations of Shull⁴¹ indicate that two brushes, when immersed in a melt of chains composed of identical monomers, can either attract or repel each other, depending on the grafting density and the ratio of chain lengths, N_f/N_g (N_f and N_g are the number of repeat units per chain of the free and grafted chains, respectively). For high grafting densities, increasing N_f/N_g leads to a crossover from repulsion to attraction. The crossover occurs at N_f/N_g values between 1 and 2. Interdomain attractions may therefore occur in systems where the molecular weight of the matrix component is larger than that of the corresponding block in the copolymer.

Results and Discussion

The electron microscopy results of ternary blends of PE, PP, and PE-PP[45-90] are shown in Figure 4. All the ternary blends were stained with RuO₄. At the bottom of Figure 4 (Figures 4 (a-c)), we show the effect of increasing the ratio of w ($w = \phi_{\text{PE-PP}}/\phi_{\text{PE}}$) from 0.53 to 3.69, keeping the dispersed phase volume fraction, ϕ ($\phi = \phi_{\text{PE-PP}} + \phi_{\text{PE}}$), fixed at 0.05. For all values of w spherical domains with apparent diameters ranging from 0.1 to $1 \mu\text{m}$ were obtained. However, two qualitative differences are evident when these domains are compared with the spheres found in binary PE/PP blends (Figure 2):

(1) The domains in the multicomponent blends are surrounded by a dark "line". We have some evidence that this line represents the copolymer chains that have migrated to the domain-matrix interface. The thickness of this line is about $0.02 \mu\text{m}$.⁴² This value is larger than the estimated (unperturbed) R_g of the PP block in the PE-PP[45-90] chains which is $0.01 \mu\text{m}$.²⁹ The thickness of the dark line is therefore consistent with that of a PP block that is stretched by a factor of 2, relative to the unperturbed state. Chain stretching is expected when block copolymer junctions are confined to the domain-matrix interface, and this is consistent with our observations. This consistency, and the fact that the dark line is absent when the blends do not contain the block copolymer (Figure 2), leads us to conclude that the line represents the diblock copolymer chains located at the domain-matrix interface.

It is evident that the diblock copolymer coat is preferentially attacked by the RuO₄. There are two possible reasons for this. First, the continuous PP-rich phase (matrix) has some PE mixed in because χ is finite and therefore resists staining, while the block copolymer layer is expected to exclude the homopolymers.⁴ Second, the residual C=C unsaturation in the block copolymer is larger than that in the PP homopolymer. Since the unsaturation was within instrumental resolution for both the PP and PE-PP[45-90], we cannot substantiate this. In any case, the preferential staining of the block copolymer chains serves as a convenient way of locating them in the multicomponent blends.

(2) Clusters of uncoalesced, spherical domains are evident in the presence of the block copolymer (Figure 4a-c). This indicates a resistance to coalescence that was not found in the absence of block copolymer (Figure

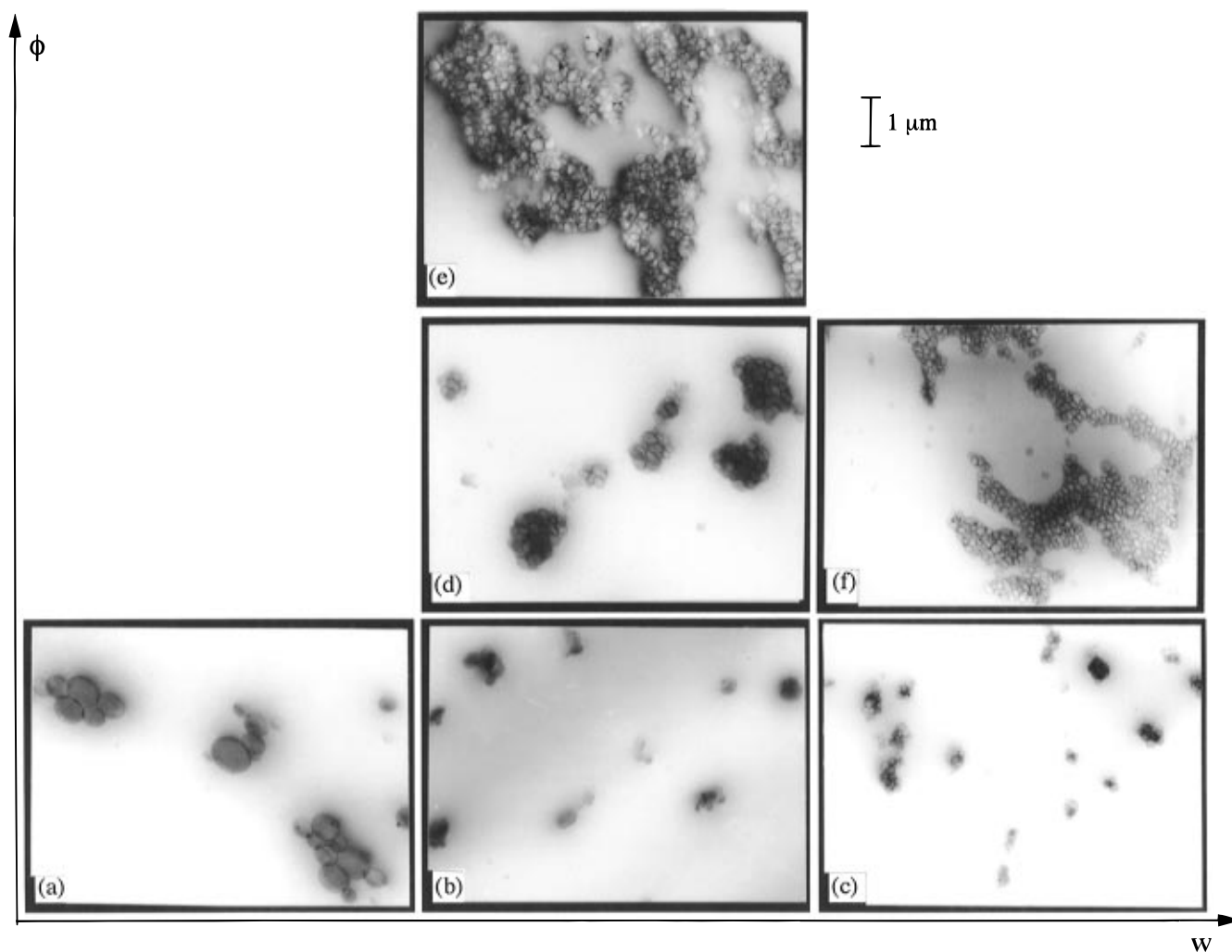


Figure 4. Typical transmission electron micrographs of PE/PP/PE-PP[45-90] blends as a function of w and ϕ . These samples were stained with RuO_4 which preferentially stains the PP block of the block copolymer: (a) $\phi = 0.05$ and $w = 0.53$, (b) $\phi = 0.05$ and $w = 2.35$, (c) $\phi = 0.05$ and $w = 3.69$, (d) $\phi = 0.10$ and $w = 2.34$, (e) $\phi = 0.16$ and $w = 2.35$, and (f) $\phi = 0.10$ and $w = 3.24$.

2). An obvious explanation for this is the presence of the block copolymer at the interface.

It is evident in Figure 4a-c that increasing w at a fixed value of $\phi = 0.05$ has little effect on the shape of the PE domains. The domain size decreases with increasing w , consistent with the well-documented compatibilization effect. However, there is no significant reduction in clustering with increasing block copolymer concentration at $\phi = 0.05$.

A dramatic transformation in domain shape is observed when ϕ is increased from 0.10 to 0.16 while keeping w fixed at 2.35 (Figure 4d,e). At $\phi = 0.10$ we find relatively small clusters of spheres, comprising, on average, 14 spheres/cluster.⁴³ When ϕ is increased to 0.16, we find that the PE domains now have a polygonal shape with faceted walls that are nearly flat. Further, the domains coalesced into large, irregularly shaped clusters containing over 10^2 domains/cluster.⁴³ The dispersed phase only occupies 16% of the volume, and thus the domain-rich regions were separated by very large, featureless PP-rich regions. The appearance of the dispersed phase is reminiscent of cellular structures found in foams and soap froth; we refer to this as the "cell-like" morphology.

Figure 4d,f shows the effect of increasing w keeping ϕ constant at 0.10. Again we see a change in domain shape from clusters of spheres to irregularly shaped clusters of cells. Usually increasing block copolymer

concentration (w) leads to a finer dispersion. This is not what we find at $\phi = 0.10$. The characteristic size (average diameter) of the spheres in the binary PE/PP blends with $\phi = 0.10$ was about $1\ \mu\text{m}$ (Figure 2).^{42,43} The characteristic size of the clusters in the multicomponent blend with $\phi = 0.10$ and $w = 3.24$ (Figure 4f) is more difficult to quantify due to their irregular shape, but it clearly is much larger than $1\ \mu\text{m}$. In binary blends the dispersed phase size will approach infinity with increasing time. The fact that the dispersed phase size in ternary PE/PP/PE-PP blends exceeds that in a binary PE/PP blend after identical thermal history indicates that the cell-like domains have strong adhesive interactions.

Our observations on blends containing PE-PP[45-90] are summarized in Figure 5 where the morphology is plotted as a function of ϕ and w . Only spheres and cell-like morphologies were observed in the range of compositions that were studied. The circles represent spherical domains, while the hatched squares represent cell-like domains. The solid curve represents the experimentally determined transition from spheres to cells. This transition from spheres-to-cells is not infinitely sharp, i.e., it is not a strongly first-order phase transition. The curve in Figure 5 is meant to differentiate samples with predominantly small clusters of spheres with curved interfaces from those with large macrophases comprising cell-like domains with predomi-

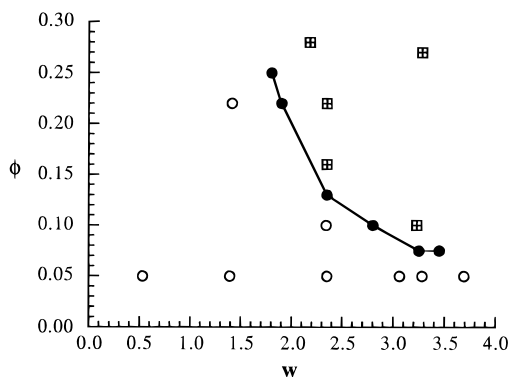


Figure 5. Summary of the observed morphology in PE/PP/PE-PP[45-90] blends as a function of w and ϕ . The circles represent blends with a spherical morphology, and the hatched squares represent blends with a cell-like morphology. The solid line represents the locations of the transition from spheres to cells.

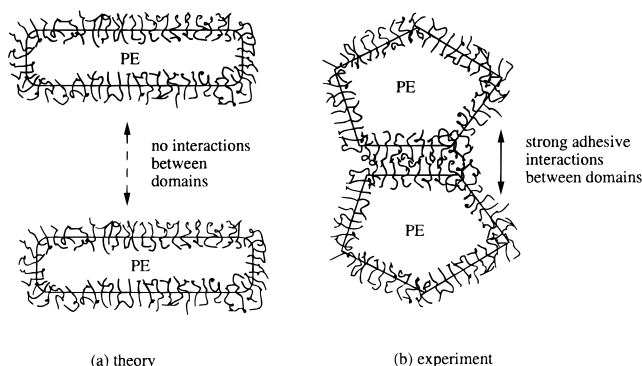


Figure 6. Schematic representation of the similarities and differences between the theoretically proposed domains with flat interfaces and those observed experimentally.

nantly flat interfaces. The distinction is not entirely clear, especially in the vicinity of the solid curve. For example, some cell-like domains can be seen at $\phi = 0.10$ and $w = 2.34$ (Figure 4d). The spherical assignment for this sample was based primarily on the fact that the domain clusters were relatively small in size.

For the system with $\phi = 0.10$, the sphere-to-cell transition occurs at $w = 2.77 \pm 0.5$. This is in reasonable agreement with the Wang-Safran prediction for the onset of the lamellar phase. In fact, the Wang and Safran treatment focused on the curvature of the block copolymer coating and concluded that for $w > 2.75$, the minimum free energy of the system occurs for zero curvature. This is consistent with what we find. The block copolymer coat is flat (or nearly so) when $w = 3.23$. However, the PE domains are not encapsulated by two block copolymer sheets. Instead, several sheets—typically 4–6—combine to confine the PE domains. The cell-like domains thus bear some resemblance to the lamellar domains proposed by Wang and Safran. In fact, within the approximations of the theory, these two structures have indistinguishable free energies. The driving force for a cell-like morphology relative to lamellae is related to edge defects. To encapsulate a lamellar domain, a narrow block copolymer coat with large curvature would be necessary. On the other hand, the intersheet curvature is relatively mild in the case of the cell-like morphology. The differences and similarities between theory and experiment are illustrated in Figure 6. The theory predicts the formation of cylindrical domains at w values between 1.77 and 2.77. We examined several blends in this range (Figure 5) but found no evidence for their existence.

The Wang-Safran theory is based on the assumption of noninteracting domains. This is a reasonable approximation for spherical domains but not for cell-like domains. In the latter case there is a strong tendency for interdomain adhesion. This leads to macrophase separation into domain-rich and domain-poor phases. The fact that the sphere-to-cell transition line in Figure 5 is not vertical also indicates the presence of interdomain interactions. There is thus a clear breakdown of the theory as the sphere-to-cell transition line is approached. Our data indicate that interdomain attraction dominates once the faceted structures are formed. The reason for this may be contained in the work of Shull,⁴¹ where interbrush attractions are predicted for N_f/N_g values between 1 and 2. The value of N_f/N_g for PE/PP/PE-PP blends containing PE-PP[45-90] is 1.1. Thus domains coated with PE-PP[45-90] in a predominantly PP matrix are at the border between repulsion and attraction. It is important to note that the brushes in our blend have extra degrees of freedom, relative to the terminally anchored brushes studied by Shull. In addition, the matrix must contain some PE that is mixed in with the PP. It is possible that these factors combine to produce interbrush attractions at lower values of N_f/N_g .

Given the similarity of the cell-like structure to soap froth and the large sizes of the macrophases, it is appropriate to question the applicability of equilibrium theories to our system. The structural evolution in soap froth is governed by nonequilibrium processes, similar to those found during grain growth in metallic systems.⁴⁴ It is conceivable that the size of the cell-like structures found in PE/PP/PE-PP[45-90] blends is determined by similar processes.

From the limited experiments that we have conducted, it appears that the adhesion is always present for the cell-like domains and does not diminish with decreasing domain concentration. Adhesion is seen to diminish only when the dispersed phase becomes spherical. Our experiments indicate a need for a more complete theory of domain shape transitions in which interdomain interactions and edge defects are included.

There are some similarities between our observation and those in oil-water microemulsions. Strey and co-workers found the existence of domain-rich and domain-poor macrophases in these systems.⁶ However, the morphology of the domains in this region of the phase diagram remains to be determined.^{5,6} Menes et al. have proposed a theory where they show that interdomain attractions can lead to this kind of phase separation.⁵ Their work was limited to cylindrical and spherical domains found in oil-water microemulsions. Our experiments indicate that these effects are important in polymer microemulsions as well and that domains with flat interfaces are more prone to interdomain attractions.

The cell-like morphology reported here is similar to that observed by Adedeji et al.¹⁸ in blends of poly(styrene-*co*-acrylonitrile) (SAN), polystyrene (PS), and poly(styrene-*b*-methyl methacrylate) (PS-PMMA). Adedeji et al. argued that specific interactions and exothermic mixing between PMMA and SAN was responsible for the cell-like morphology. We demonstrate here that such morphologies can be obtained in polyolefin blends without specific interactions.

We now turn to blends containing PE-PP[115-65]. Typical morphologies of these blends are shown in Figure 7. The effect of increasing w while keeping ϕ fixed at 0.05 is shown at the bottom of Figure 7a-c. At

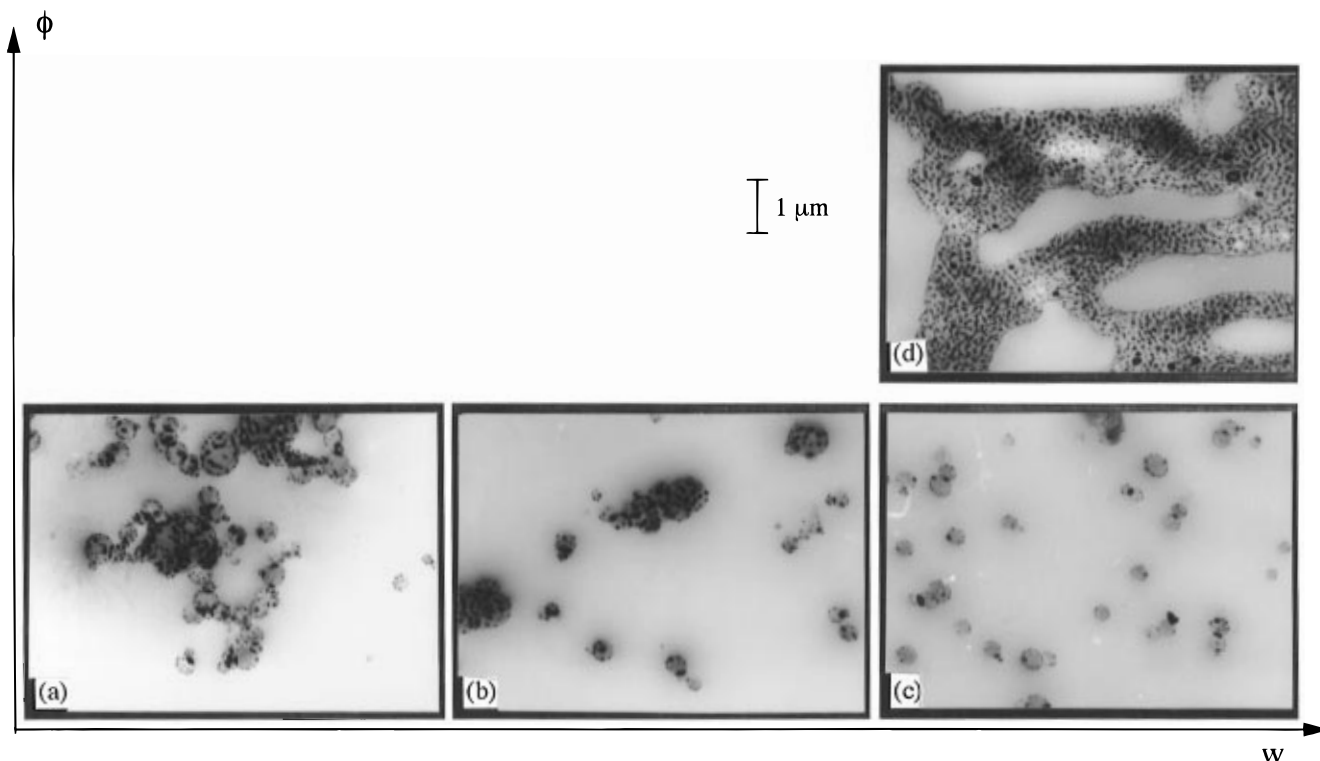


Figure 7. Typical transmission electron micrographs of PE/PP/PE-PP[115-65] blends as a function of w and ϕ . These samples were stained with RuO_4 which preferentially stains the PP block of the copolymer: (a) $\phi = 0.05$ and $w = 1.40$, (b) $\phi = 0.05$ and $w = 1.96$, (c) $\phi = 0.05$ and $w = 3.24$, and (d) $\phi = 0.33$ and $w = 3.24$.

low values of w we find coalesced spheres with a dark outline, representing the copolymer located at the interface. This is similar to what was observed in the blends containing PE-PP[45-90]. However, there is an important difference. In the PE-PP[115-65] blends we find that the spherical PE phase contains small, dark spheres. The apparent radius of the spheres ranges from 0.01 to 0.04 μm , with an average value of 0.028 μm .^{42,43} We compare this to the dimension of the PP block in the ordered PE-PP[115-65] material, which is 0.019 μm (equal to $d(1 - f)/2$), and the unperturbed dimension of the PP block, which is 0.010 μm . The size of the dark spheres within the PE phase are consistent with the notion that the PE-PP[115-65] chains form micelles with a PP core and a PE corona. The dark regions represent the PP core. Theories on micelle formation in block copolymers indicate that chains in the core of the micelle are stretched relative to their unperturbed dimension.⁴⁵ Our observations are consistent with this prediction. It is also possible that the larger micelles (with radii in the vicinity of 0.04 μm) contain some solubilized PP homopolymer. Regardless of blend composition, the micelles are located exclusively in the PE phase. This may be due to the fact that PE is the major component in the block copolymer.

We find that PE-PP[115-65] is not an effective compatibilizer at low values of w because instead of assembling at the interface most of the copolymer segregates within the PE phase in the form of micelles. At $w < 3.24$ we find large clusters of PE spheres (Figure 7a,b). However, the size of the clusters decreases with increasing w . At $w = 3.24$ we find that the PE phase formed a very fine spherical dispersion with relatively few block copolymer micelles. Most of the micelles are located at the domain-matrix interface. We see no evidence of domain shape transitions when the PE-PP[115-65] block copolymer is used. In particular, no cell-

like structures were found in the range $0.05 < w < 3.28$.

We thought that, perhaps, increasing ϕ at constant w may cause a sphere-to-cell transition, as was the case with the PE-PP[45-90] system. We thus examined a blend with $\phi = 0.33$ and $w = 3.28$. Instead of the cell-like morphology, we found an irregularly shaped macrophase of PE with block copolymer micelles within. We thus find that the domain shape transitions are sensitive to the molecular weight and architecture of the block copolymer. In particular, changing the block copolymer from PE-PP[45-90] to PE-PP[115-65] leads to micelle formation. This, in turn, seems to inhibit domain shape transitions.

Concluding Remarks

We have conducted a systematic study of domain shapes in phase-separated mixtures of PE, PP, and PE-PP diblock copolymers with PE as the minor component. Our experiments were designed to obtain the morphology of the blends at 200 $^{\circ}\text{C}$. All the components are amorphous and in the rubbery state at this temperature. The objective was to examine the possibility of domain shape transitions that were proposed by Wang and Safran.⁴ Blend morphology was studied as a function of two variables: (1) the overall dispersed phase volume fraction, ϕ , and (2) the block copolymer volume concentration relative to the minor component, w . We examined two series of ternary PE/PP/PE-PP mixtures, one containing PE-PP[45-90] and the other containing PE-PP[115-65].

We found that the emulsifying capability of PE-PP[115-65] was diminished due to micelle formation, and we did not observe any change in the shape of the PE domains. On the other hand, the PE-PP[45-90]-containing blends showed a dramatic domain shape transition from spherical to cell-like structures for blends with $\phi \geq 0.10$. The experimentally determined

transition from spheres to cells at $\phi = 0.10$ occurred at $w = 2.8$. This transition is in the vicinity of the point at which the theory of Wang and Safran predicts the formation of domains with flat walls. The cell-like structures that we have identified have flat walls. However, the cells exhibited strong attractive interactions, while the theory assumes noninteracting domains. It is therefore not entirely clear if the underpinnings of the experimentally observed domain shape transitions are captured by the theory. Other predictions, such as the existence of cylindrical domains at intermediate block copolymer concentrations, are not borne out by experiments.

We suggest that interdomain attractions in these systems may be similar to those between grafted brushes.⁴¹ It is likely that this attraction will depend on brush density, which, in turn, is determined by interactions between PP and PE chains, i.e., the magnitude of the χ parameter. The current theory⁴ is independent of χ for large χN . Perhaps, a more quantitative measure of χ may be useful. We are conducting small angle neutron scattering experiments on low molecular weight PE and PP homopolymer mixtures, and a preliminary estimate of χ is available.²⁴ Due to the temperature dependence of χ , we may observe thermally induced structural changes. Changing temperature in oil–water microemulsions leads to reentrant phase transitions.^{5,6} Our future experiments will be along these lines. We hope, however, that our results thus far will provide the incentive for refining current theories^{3,4} on domain shape transitions in emulsified polymer blends.

Acknowledgment. Financial support from the National Science Foundation to Polytechnic University (CTS-9308164, DMR-9307098, and DMR-9457950), the 3M Non-Tenured Faculty Award to N.P.B., and the Exxon Education Foundation is gratefully acknowledged. We thank John Kremers, Pratima Rangarajan, Charles Ruff, Frank Radden, Glenn Reichart, and Lachman Soni for their help in the characterization of these materials, Bill Graessley, Sam Safran, Ken Shull, and Zhen-Gang Wang for helpful discussions, and the reviewers for useful suggestions.

Nomenclature

f	volume fraction of PE in block copolymer
G_n^0	plateau modulus (MPa)
N	number of repeat units per polymer chain
N_f	number of repeat units per chain of the free chains in contact with a brush
N_g	number of repeat units per chain of the grafted chains in a brush
PE	homopolymer polyethylene
PP	homopolymer head-to-head polypropylene
PE–PP	diblock copolymer with PE and PP blocks
R_g	radius of gyration (Å)
w	ratio of block copolymer volume fraction to minor homopolymer volume fraction ($w = \phi_{\text{PE-PP}}/\phi_{\text{PE}}$)
χ	Flory–Huggins interaction parameter
ϕ	dispersed phase volume fraction ($\phi = \phi_{\text{PE-PP}} + \phi_{\text{PE}}$)
ϕ_i	volume fraction of component i ($i = \text{PE, PP, and PE-PP}$)
η_0	zero shear viscosity
τ	relaxation time (s)

References and Notes

- (1) de Gennes, P. G.; Taupin, C. *J. Phys. Chem.* **1982**, *86*, 2294 and references therein.
- (2) Roe, R. J.; Rigby, D. *Adv. Polym. Sci.* **1987**, *82*, 103 and references therein.
- (3) Leibler, L. *Makromol. Chem. Macromol. Symp.* **1988**, *16*, 1.
- (4) Wang, Z. G.; Safran, S. A. *J. Phys. (France)* **1990**, *51*, 185.
- (5) Menes, R.; Safran, S. A.; Streyl, R. *Phys. Rev. Lett.* **1995**, *74*, 3399.
- (6) Kahlweit, M.; Streyl, R.; Busse, G. *J. Phys. Chem.* **1990**, *94*, 3881.
- (7) Milner, S. T.; Witten, T. *J. Phys. (France)* **1988**, *49*, 1951.
- (8) Huggins, M. L. *J. Chem. Phys.* **1941**, *9*, 440.
- (9) Flory, P. J. *J. Chem. Phys.* **1941**, *9*, 660.
- (10) Balsara, N. P. In *Physical Properties of Polymers Handbook*; Mark, J. E., Ed.; AIP Press: New York, 1996; Chapter 19 and references therein.
- (11) Lin, C. C.; Jonnalagadda, S. V.; Balsara, N. P.; Han, C. C.; Krishnamoorti, R. *Macromolecules* **1996**, *29*, 661.
- (12) Balsara, N. P.; Jonnalagadda, S. V.; Lin, C. C.; Han, C. C.; Krishnamoorti, R. *J. Chem. Phys.* **1993**, *99*, 10011.
- (13) Lin, C. C.; Jeon, H. S.; Balsara, N. P.; Hammouda, B. *J. Chem. Phys.* **1995**, *103*, 1957.
- (14) Lin, C. C.; Jonnalagadda, S. V.; Kesani, P. K.; Dai, H. J.; Balsara, N. P. *Macromolecules* **1994**, *27*, 7769.
- (15) Ramos, A. R.; Cohen, R. E. *Polym. Sci. Eng.* **1977**, *17*, 639.
- (16) Beck Tan, N. C.; Tai, S. K.; Briber, R. M. *Polymer* **1996**, *37*, 3509.
- (17) Milner, S. T.; Xi, H. *J. Rheol.*, in press.
- (18) Adedeji, A.; Jamieson, A. M.; Hudson, S. D. *Macromolecules* **1995**, *28*, 5255.
- (19) Lohse, D. J.; Datta, S.; Kresge, E. N. *Macromolecules* **1991**, *24*, 561.
- (20) Rachapudy, H.; Smith, G. G.; Raju, V. R.; Graessley, W. W. *J. Polym. Sci., Polym. Phys. Ed.* **1979**, *17*, 1211.
- (21) Morton, M.; Fetters, L. J. *Rubber Chem. Tech.* **1975**, *48*, 359.
- (22) Horská, J.; Stejskal, J.; Kratochvil, P. *J. Appl. Polym. Sci.* **1983**, *28*, 3873.
- (23) Separate aliquots of the polydiene precursors of PE–PP[45–90] and PE–PP[115–65] were saturated with H₂ and D₂ because we were planning to use these materials in small angle neutron scattering studies. All the characteristics reported in this paper refer to the hydrogenated components. However, all the blends studied in this paper contained the partially deuterated block copolymers. The presence of deuterium labels on the block copolymers is irrelevant to the present study. The average number of D atoms per C₆ repeat unit is about 5 for both PE–PP[45–90] and PE–PP[115–65].
- (24) The effect of 1–4 mol % incorporation in polydienes on χ between the polyolefins obtained by saturating them has been systematically investigated in the case of polybutadiene. The χ parameter between polyolefins obtained from 92% 1,4-butadiene and 75% 1,4-butadiene is 5.6×10^{-4} at 167 °C (the highest temperature at which this system was studied).¹⁰ Preliminary SANS experiments on PE/PP homopolymers by Balsara and Jeon (unpublished) indicate that χ between these polymers is 6.4×10^{-3} at 167 °C. We are not aware of any direct measurements of χ between polyolefins obtained from 2,3-dimethylbutadiene. The χ parameter between PE and PP units is therefore 1 order of magnitude larger the estimated effect of microstructure mismatch. The χ parameters reported here are based on a reference volume of 100 Å³.
- (25) The amorphous densities, ρ , of the components, used to calculate blend composition are $\rho_{\text{PE}} = 0.856 \text{ gm/cm}^3$, $\rho_{\text{PP}} = 0.874 \text{ g/cm}^3$, $\rho_{\text{PE-PP[45-90]}} = 0.925 \text{ g/cm}^3$, and $\rho_{\text{PE-PP[115-65]}} = 0.919 \text{ g/cm}^3$. The high densities of the block copolymers are due to the presence of deuterium labels.
- (26) Krigas, T. M.; Carella, J. M.; Struglinski, M. J.; Crist, B.; Graessley, W. W.; Schilling, F. C. *J. Polym. Sci., Polym. Phys. Ed.* **1985**, *23*, 509.
- (27) Carella, J. M.; Graessley, W. W.; Fetters, L. J. *Macromolecules* **1984**, *17*, 2775.
- (28) Gell, C. Ph.D. Thesis, Princeton University, 1996.
- (29) Fetters, L. J.; Lohse, D. J.; Richter, D.; Witten, T. A.; Zirkel, A. *Macromolecules* **1994**, *27*, 4639.
- (30) Hajduk, D. A.; Harper, P. E.; Gruner, S. M.; Honeker, C. C.; Kim, G.; Thomas, E. L.; Fetters, L. J. *Macromolecules* **1994**, *27*, 4063.
- (31) Nojima, S.; Kato, K.; Yamamoto, S.; Ashida, T. *Macromolecules* **1992**, *25*, 2237.
- (32) Khandpur, A. K.; Macosko, C. W.; Bates, F. S. *J. Polym. Sci., Polym. Phys. Ed.* **1995**, *33*, 247.
- (33) Cohen, R. E.; Cheng, P. L.; Douzinas, K.; Kofinas, P.; Berney, C. V. *Macromolecules* **1990**, *23*, 324.

- (34) Rangarajan, P.; Register, R. A.; Fetters, L. J.; Bras, W.; Naylor, S.; Ryan, A. J. *Macromolecules* **1995**, *28*, 4932.
- (35) Leibler, L. *Macromolecules* **1980**, *13*, 1602.
- (36) Roe, R. J.; Zin, W. C. *Macromolecules* **1984**, *17*, 189.
- (37) de Gennes, P. G. *Scaling Concepts in Polymer Physics*; Cornell University Press: Ithaca, NY, 1979.
- (38) Hadziannou, G.; S. Patel, S.; Granick, S.; Tirrell, M. *J. Am. Chem. Soc.* **1986**, *108*, 2869.
- (39) Alexander, S. *J. Phys.* **1977**, *38*, 983.
- (40) Milner, S. T.; Witten, T. A.; Cates, M. E. *Macromolecules* **1988**, *21*, 2610.
- (41) Shull, K. *J. Chem. Phys.* **1991**, *94*, 5723.
- (42) The size of these features was estimated by digitizing the micrograph with an EPSON 1300 scanner and using Adobe Photoshop to magnify the image.
- (43) The number-average number of domains per cluster was obtained by examining several micrographs, covering an area ranging from 70 to 200 μm^2 per sample.
- (44) Wejchert, J.; Weaire, D.; Kermode, J. P. *Philos. Mag. B* **1986**, *53*, 15.
- (45) Leibler, L.; Orland, H.; Wheeler, J. C. *J. Chem. Phys.* **1983**, *79*, 3550.

MA961232E